科学通报 2019 年 第 64 卷 第 12 期: 1303 ~ 1308
专题: 激光制造结构化仿生表面 论 文
《中国科学》杂志社
SCIENCE CHINA PRESS

激光加工制备仿芦苇叶结构的超疏水表面

陈峒霖[1], 毛江维[1], 陈招弟[1], 于凯新[1], 韩冬冬[1], 孙洪波[1,2*]

1. 吉林大学电子科学与工程学院, 集成光电子学国家重点联合实验室, 长春 130012;
2. 清华大学精密仪器系, 精密测试技术及仪器国家重点实验室, 北京 100084
* 联系人, E-mail: hbsun@tsinghua.edu.cn

2018-08-24 收稿, 2018-09-27 修回, 2018-10-14 接受, 2018-11-13 网络版发表
国家重点研发计划(2017YFB1104300)、国家自然科学基金(61522503, 61590930, 61775078 和 61605055)和吉林省科技发展计划(20180101061JC)资助

摘要 仿芦苇叶结构的超疏水表面在抗结冰、自清洁等领域有着重要的应用. 但是, 目前仍缺乏一种简单制备仿芦苇叶微纳米结构的方法. 本文采用激光烧蚀手段制备基于聚二甲基硅氧烷的具有仿芦苇叶结构超疏水表面. 激光烧蚀处理具有微光栅结构的聚二甲基硅氧烷, 高能量激光作用时可以烧蚀出次级微纳结构, 提高表面粗糙度, 其浸润性各向异性明显, 沿着垂直方向测量的接触角(~155°)比平行方向测量的接触角(~150°)大, 达到超疏水, 且沿着垂直方向测量的滚动角(~3°)比平行方向测量的接触角(~12°)小. 本方法为激光制备仿生结构超疏水表面提供了新思路.

关键词 激光制造, 仿生, 芦苇叶, 超疏水, 聚二甲基硅氧烷

在自然演化的过程中, 生物进化出许多独特的结构与性质, 比如: 蝴蝶翅膀由于具有微纳米级的光栅结构, 看起来色彩缤纷; 荷叶表面由于具有微纳突起结构, 具有超疏水自清洁现象等[1]. 因此, 科研人员一直尝试通过不同方法制备与生物模板表面相近的结构, 进而实现特定功能[2~5]. 以超疏水现象为例, 中国科学技术大学吴东课题组[6]利用聚二甲基硅氧烷(PDMS)转写微光栅结构, 随后在PDMS光栅结构表面黏附超疏水材料, 制备仿水稻叶超疏水表面. 吉林大学刘燕课题组通过电沉积方法在镁合金[7]和铜[8]表面制备仿生微纳结构, 实现超疏水特性. 近年来, 激光加工具有精度高、任意加工等优点, 在仿生制造领域显示出巨大的优势[9~12]. 如西安交通大学陈烽课题组利用飞秒激光在硅表面加工菱形、三角形、圆形微图案[13], 在PDMS表面制备微"井"阵列[14]、网格阵列[15]、阶梯结构[16]调节表面液滴黏附性. 本课题组先后利用激光直写微纳结构[17]、双光束干涉[18,19]和四光束干涉[20]等技术方法制备微纳复合多级结构, 实现超疏水表面的制备. 虽然这些方法成功制备超疏水表面, 但是主要依靠复杂精密的仪器设备, 而且制备大面积超疏水表面加工过程时间较长.

本文首先利用PDMS转写微米结构的模板, 获得周期为微米量级的PDMS光栅结构. 然后利用二氧化碳激光器烧蚀PDMS微结构表面, 引入纳米结构. 最终, 制备类似芦苇叶的微纳复合结构, 实现超疏水功能, 并证明浸润性的各向异性. 该方法简单、方便、成本低, 有可能成为制备超疏水表面的通用方法.

1 实验与表征

PDMS(Sylgard 184 Silicone Elastomer, Dow Corning Corporation), 固化剂以质量比10:1混合, 95℃固化1 h. 二氧化碳激光器(JW6090, JG. 山东), 扫描速度100 mm/s, 步长0.03 mm.

X射线光电子能谱(XPS, ESCALAB 250 spectro-

引用格式: 陈峒霖, 毛江维, 陈招弟, 等. 激光加工制备仿芦苇叶结构的超疏水表面. 科学通报, 2019, 64: 1303–1308
Chen D L, Mao J W, Chen Z D, et al. Fabrication of bionic reed leaf superhydrophobic surface by laser processing (in Chinese). Chin Sci Bull, 2019, 64: 1303–1308, doi: 10.1360/N972018-00872

© 2018《中国科学》杂志社

meter)测试样品表面元素变化，激光共聚焦显微镜(CLS, OLS4100)和扫描电子显微镜(SEM, JSM-7500)测试样品表面形貌变化，接触角仪器(SL200B, Solon Tech.)测试样品表面水滴接触角数值变化.

2 结果与讨论

2.1 激光对PDMS改性

首先利用激光共聚焦显微镜对芦苇叶表面进行观测. 图1(a)为芦苇叶的激光共聚焦照片，芦苇叶表面具有百微米周期的条纹结构. 进一步提高放大倍数，可以发现芦苇叶微米条纹表面具有许多微纳米级的次级结构(图1(b))，我们可以将芦苇叶表面超疏水现象归结为百微米周期条纹光栅表面分布微纳米级的突起.

由于PDMS具有优秀的转写复形能力，我们将固化剂充分混合的PDMS倾倒在周期型的凹槽表面，放置在95℃烘箱1 h，使PDMS充分填充到凹槽内部并固化. 固化1 h后，将PDMS从烘箱中取出，待降至室温，再小心将PDMS从模板表面揭下来备用，获得的PDMS具有周期光栅条纹结构.

接下来，如图1(c)所示，利用二氧化碳激光器烧蚀有条纹结构的PDMS表面. 激光烧蚀PDMS表面使PDMS碳化，产生微纳米级的突起，提高表面粗糙程度. 利用激光共聚焦显微镜分别测试PDMS、激光烧蚀之后的PDMS和激光烧蚀条纹结构的PDMS的粗糙度，粗糙度分别为0.280, 13.371和18.781 μm，条纹结构的引入使得表面粗糙度提高. 粗糙度的提高是表面浸润性改变的主要原因[15].

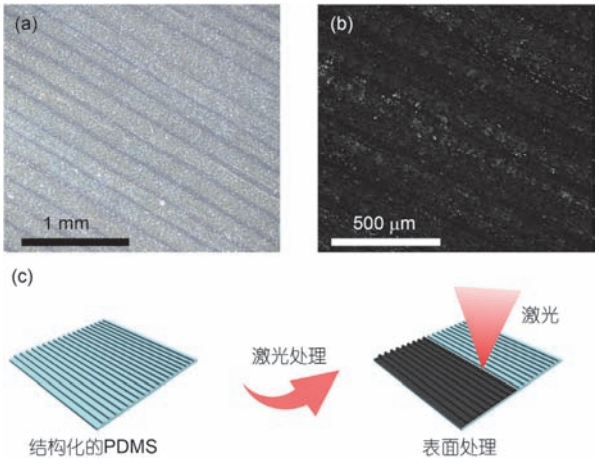


图 1 (网络版彩色)芦苇叶激光共聚焦显微镜照片(a, b)和激光制备仿生芦苇叶(c)的示意图

Figure 1 (Color online) (a, b) CLSM images of reed leaves. (c) Schematic illustration of fabrication of reed leaf by laser treatment

2.2 激光改性的PDMS基本表征

为了分析激光对PDMS烧蚀前后元素含量的变化，分别对PDMS和激光烧蚀后的PDMS进行XPS测试. 如图2所示，激光作用前，PDMS的碳元素含量为43.6%，激光作用后，碳元素含量减少至33.1%. 与此同时，激光作用后，氧元素的含量从27.8%提高到33.6%，硅元素含量从28.3%提高到33.3%. 碳元素含量的减少说明在激光处理过程中，有碳物质的排放，这是由PDMS表面的甲基被碳化造成的. 激光处理过的PDMS表面积碳会诱导材料表面变黑，改变其表面能[21~23].

为了对比激光作用前后PDMS表面结构形貌的变化，分别对激光处理前后PDMS条纹表面形貌利用激光共聚焦显微镜进行观察. 图3(a), (b)为初始条纹结构的PDMS激光共聚焦照片，条纹宽度约100 μm，高度约130 μm，结构表面光滑. 图3(c), (d)为激光烧蚀的分界位置，经过激光烧蚀之后，PDMS变得更为粗糙. 图3(c), (d)为激光烧蚀后的PDMS，条纹宽度约200 μm，高度约110 μm，表面更为粗糙. 激光烧蚀后，PDMS条纹宽度和高度的变化主要是由于激光处理使得PDMS表面材料碳化出粗糙结构.

为了进一步详细观察样品表面形貌，利用SEM对样品激光烧蚀前后的形貌进行表征. 图4(a), (b)为初始PDMS的SEM照片和局部放大照片，整个PDMS表面较为光滑. 图4(c), (d)为激光处理之后的PDMS表面，通过与初始PDMS的SEM照片对比，结果表明经过激光烧蚀后的PDMS表面由于碳化出现微米和纳米级结构，微纳结构的出现有利于提高表面的浸

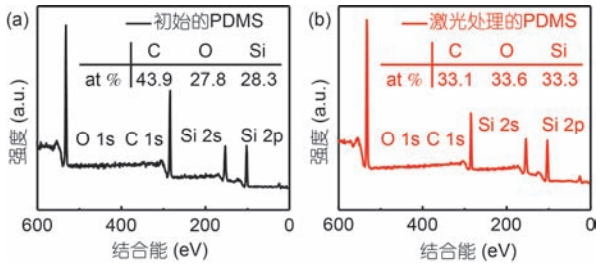


图 2 (网络版彩色)PDMS(a)和激光处理后PDMS(b)的XPS谱图

Figure 2 (Color online) XPS spectra of the pristine (a) and treated PDMS (b)

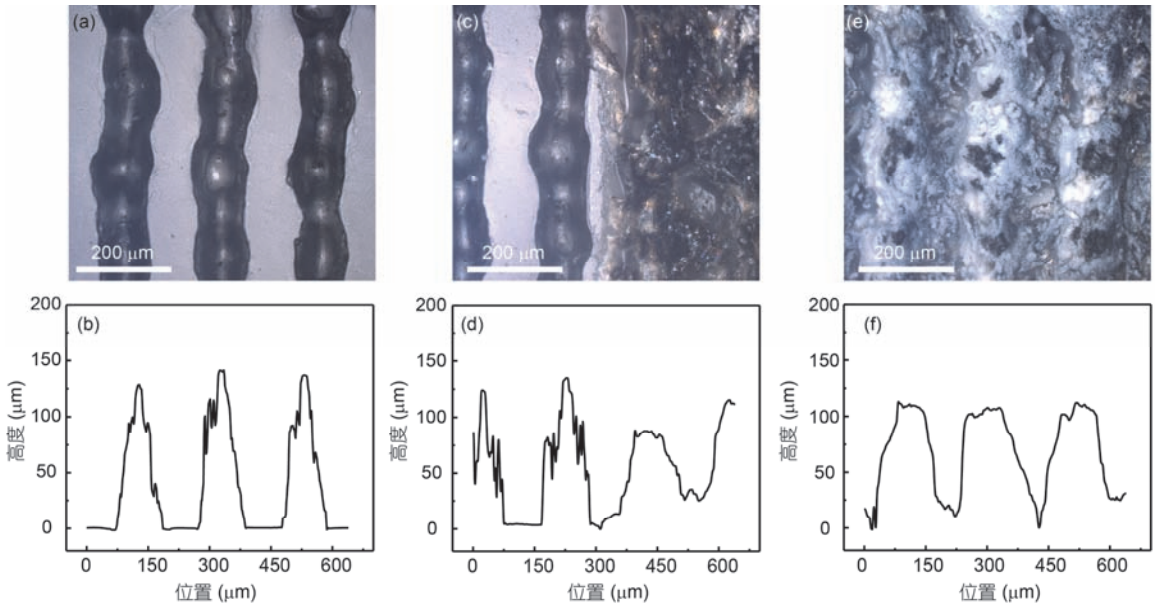


图 3 (网络版彩色)PDMS条纹的激光共聚焦显微镜照片(a)和剖面高度曲线(b); 初始PDMS与激光处理过的PDMS部分的激光共聚焦显微镜照片(c)及相应的剖面高度曲线(d); 激光处理过的PDMS的激光共聚焦显微镜照片(e)和高度曲线(f)

Figure 3 (Color online) CLSM images (a) and height profile (b) of structured PDMS. CLSM images (c) and height profile (d) of the boundary between structured PDMS and laser treated structured PDMS. CLSM images (e) and height profile (f) of laser treated structured PDMS

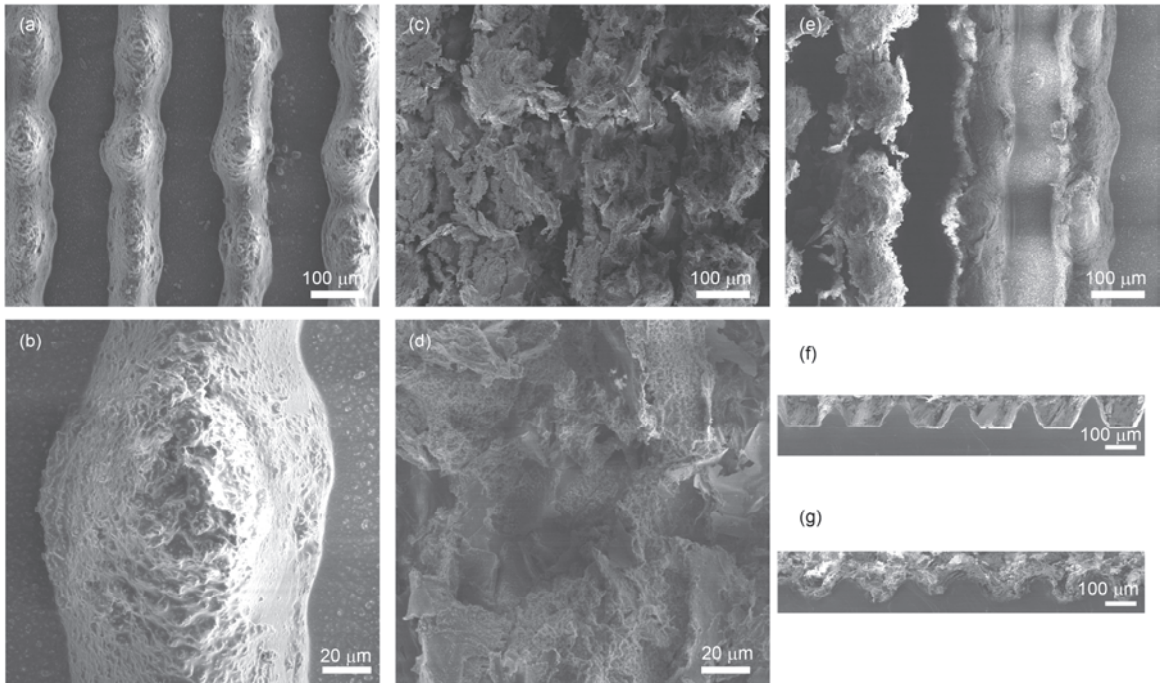


图 4 初始PDMS(a, b)和激光处理后的PDMS(c, d)的SEM照片. (e) 初始PDMS与激光处理过的PDMS边界的SEM照片. 初始PDMS(f)和激光处理过的PDMS(g)的截面SEM照片

Figure 4 SEM images of the structured PDMS (a, b) and laser treated structured PDMS (c, d). (e) SEM images of the boundary between structured PDMS and laser treated structured PDMS. Cross section SEM images of structured PDMS (f) and laser treated structured PDMS (g)

润性. 图4(e)为原始PDMS和激光烧蚀区域的分界线, 可以更直观地观测表面处理前后的变化. 图4(f), (g)分别为初始PDMS和激光烧蚀之后的PDMS截面SEM照片, 激光作用后, PDMS碳化过程中使得条纹变宽

以及条纹高度变小.

2.3 浸润性测试

为了评估样品表面浸润性的变化, 分别对平整的PDMS, 条纹结构PDMS和激光处理过条纹结构PDMS进行水滴的接触角测量. 如图5所示, 平整的PDMS的水滴接触角约125.2°, 具有条纹结构的PDMS水滴接触角约139.8°, 经激光处理后, 水滴接触角达到155.5°, 实现超疏水. 为了进一步分析条纹结构PDMS经激光烧蚀后表面对水相浸润的各向异性, 分别对平行于条纹和垂直于条纹方向进行表面浸润性测试. 测试结果表明, 沿着垂直方向测量的接触角(~155.5°)比平行方向测量的接触角(~150°)大. 为进一步分析条纹对水相各向异性的滚动特性, 分别对平行于条纹和垂直于条纹方向进行表面滚动角测试. 测试结果表明, 沿垂直方向测量的滚动角(~3°)比平行方向测量的接触角(~12°)小.

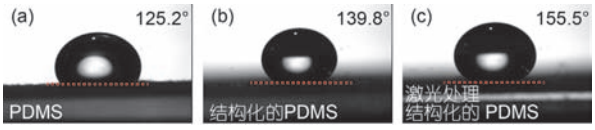


图 5 (网络版彩色)PDMS(a), 结构化的PDMS(b)和激光处理过的结构化的PDMS(c)的水滴接触角

Figure 5 (Color online) Water droplet contact angles of PDMS (a), structured PDMS (b), and laser treated structured PDMS (c)

3 总结

本文通过激光烧蚀带有条纹结构的PDMS表面直接制备类似于仿芦苇叶结构的超疏水表面. 激光烧蚀过程使得PDMS中碳元素含量降低、氧和硅元素含量升高, 提高粗糙度, 其浸润性各向异性明显, 沿着垂直方向测量的接触角(~155°)比平行方向测量的接触角(~150°)大, 达到超疏水, 且沿着垂直方向测量的滚动角(~3°)比平行方向测量的接触角(~12°)小. 该方法利用二氧化碳激光器, 设备较为便宜, 可以为仿芦苇叶结构超疏水表面的低成本、大批量、大面积制备提供思路.

参考文献

1 Zhang Y L, Xia H, Kim E, et al. Recent developments in superhydrophobic surfaces with unique structural and functional properties. Soft Matter, 2012, 8: 11217–11231

2 Han D D, Zhang Y L, Liu Y, et al. Bioinspired graphene actuators prepared by unilateral UV irradiation of graphene oxide papers. Adv Funct Mater, 2015, 25: 4548–4557

3 Han D D, Zhang Y L, Jiang H B, et al. Moisture-responsive graphene paper prepared by self-controlled photoreduction. Adv Mater, 2015, 27: 332–338

4 Wang J N, Zhang Y L, Liu Y, et al. Recent developments in superhydrophobic graphene and graphene-related materials: From preparation to potential applications. Nanoscale, 2015, 7: 7101–7114

5 E J Q, Jin Y, Deng Y W, et al. Wetting models and working mechanisms of typical surfaces existing in nature and their application on superhydrophobic surfaces: A review. Adv Mater Interfaces, 2018, 5: 39

6 Wu D, Wang J N, Wu S Z, et al. Three-level biomimetic rice-leaf surfaces with controllable anisotropic sliding. Adv Funct Mater, 2011, 21: 2927–2932

7 Liu Y, Yin X M, Zhang J J, et al. A electro-deposition process for fabrication of biomimetic super-hydrophobic surface and its corrosion resistance on magnesium alloy. Electrochim Acta, 2014, 125: 395–403

8 Liu Y, Li S Y, Zhang J J, et al. Corrosion inhibition of biomimetic super-hydrophobic electrodeposition coatings on copper substrate. Corrosion Sci, 2015, 94: 190–196

9 Jiang L, Wang A D, Li B, et al. Electrons dynamics control by shaping femtosecond laser pulses in micro/nanofabrication: Modeling, method, measurement and application. Light Sci Appl, 2018, 7: 17134

10 Chen T H, Fardel R, Arnold C B. Ultrafast z-scanning for high-efficiency laser micro-machining. Light Sci Appl, 2018, 7: 9

11 Wang L, Chen Q D, Cao X W, et al. Plasmonic nano-printing: Large-area nanoscale energy deposition for efficient surface texturing. Light Sci Appl, 2017, 6: e17112

12 Han D D, Zhang Y L, Ma J N, et al. Light-mediated manufacture and manipulation of actuators. Adv Mater, 2016, 28: 8328–8343

13 Zhang D S, Chen F, Yang Q, et al. A simple way to achieve pattern-dependent tunable adhesion in superhydrophobic surfaces by a femtosecond laser. ACS Appl Mater Interfaces, 2012, 4: 4905–4912

14 Yong J L, Chen F, Yang Q, et al. Controllable adhesive superhydrophobic surfaces based on PDMS microwell arrays. Langmuir, 2013,

29: 3274–3279
15 Yong J L, Chen F, Yang Q, et al. Femtosecond laser weaving superhydrophobic patterned PDMS surfaces with tunable adhesion. J Phys Chem C, 2013, 117: 24907–24912
16 Yong J L, Yang Q, Chen F, et al. Superhydrophobic PDMS surfaces with three-dimensional (3D) pattern-dependent controllable adhesion. Appl Surface Sci, 2014, 288: 579–583
17 Jiang H B, Zhang Y L, Liu Y, et al. Bioinspired few-layer graphene prepared by chemical vapor deposition on femtosecond laser-structured cu foil. Laser Photon Rev, 2016, 10: 441–450
18 Jiang H B, Zhang Y L, Han D D, et al. Bioinspired fabrication of superhydrophobic graphene films by two-beam laser interference. Adv Funct Mater, 2014, 24: 4595–4602
19 Jiang H B, Liu Y Q, Zhang Y L, et al. Reed leaf-inspired graphene films with anisotropic superhydrophobicity. ACS Appl Mater Interfaces, 2018, 10: 18416–18425
20 Abid M I, Wang L, Chen Q D, et al. Angle-multiplexed optical printing of biomimetic hierarchical 3D textures. Laser Photon Rev, 2017, 11: 6
21 Wang W, Liu Y Q, Liu Y, et al. Direct laser writing of superhydrophobic PDMS elastomers for controllable manipulation via marangoni effect. Adv Funct Mater, 2017, 27: 8
22 Farshchian B, Gatabi J R, Bernick S M, et al. Laser-induced superhydrophobic grid patterns on PDMS for droplet arrays formation. Appl Surface Sci, 2016, 396: 359
23 Armyanov S, Stankova N E, Atanasov P A, et al. XPS and μ-Raman study of nanosecond-laser processing of poly(dimethylsiloxane) (PDMS). Nuclear Inst Methods Phys Res B, 2015, 360: 30–35

Summary for “激光加工制备仿芦苇叶结构的超疏水表面”

Fabrication of bionic reed leaf superhydrophobic surface by laser processing

Dong-Lin Chen[1], Jiang-Wei Mao[1], Zhao-Di Chen[1], Kai-Xin Yu[1], Dong-Dong Han[1] & Hong-Bo Sun[1,2*]

[1] *State Key Laboratory on Integrated Optoelectronics, College of Electronic Science and Engineering, Jilin University, Changchun 130012, China;*
[2] *State Key Lab of Precision Measurement Technology and Instruments, Department of Precision Instrument, Tsinghua University, Beijing 100084, China*
* Corresponding author, E-mail: hbsun@tsinghua.edu.cn

In the natural evolution, animals and plants have evolved many unique structures and properties. For example, butterfly wings appear to be colorful due to grating structures. Lotus leaves have super-hydrophobic property because of micro/nano-structures. Nepenthes pitcher plants show slippery wettability by reason of the lubricant infused surfaces. Therefore, more and more researchers are trying to prepare unique structures which are similar to the surface of biological templates by different methods. Taking superhydrophobic surfaces as an example, there are many methods having been adopted to achieve superhydrophobic surfaces, such as etching, template method, UV lithography, electrostatic spinning, and nano-imprint technique. In recent years, laser processing technique has the advantages of high precision and arbitrary design, which shows great advantages in bionic manufacturing. For example, various kinds of micro/nano composites or structures have been successfully prepared by laser direct writing, two/four-beam interference, etc. However, these methods rely mainly on complex or sophisticated instruments, which take long time to prepare large-area superhydrophobic surfaces.

Reed leaves show anisotropic superhydrophilicity property because of grating structures, which has applications in droplet transmission without loss and directional collection. Herein, we demonstrated the fabrication of bionic reed leaf by laser treatment of structured polydimethylsiloxane (PDMS) surface. Laser treatment of PDMS with micro-grating structures can induce the micro-nano structures and improve the surface roughness. To investigate the change of surface chemical composition, we carried out X-ray photoelectron spectroscopy (XPS) of PDMS before and after the laser treatment. After the laser treatment, the carbon content was decreased from 43.6% to 33.1%. The decrease in carbon content indicates the emission of carbon material during laser treatment, which is caused by the carbonization of the methyl group on the surface of the PDMS. At the same time, the oxygen content increased from 27.8% to 33.6% and the silicon content increased from 28.3% to 33.3%. To compare the surface morphologies changes of PDMS before and after laser treatment, we observed the surface morphology by confocal laser scanning microscopy (CLSM) and scanning electron microscope (SEM). The initial PDMS grating is about 100 μm wide, ~130 μm high and the structure surface is smooth. After laser treatment, it changes to about 200 μm wide, ~110 μm high and becomes much rougher surface. The variation in the width and height is mainly because that the laser treatment causes PDMS surface material to carbonize into rough structures. In order to evaluate the wettability changes of samples, the static water contact angle and dynamic water sliding angle measurement was carried out on the flat PDMS, the structured PDMS, and the laser-treated structured PDMS, respectively. The contact angle along the parallel direction was ~155°, which is larger than that along the vertical direction (~150°). The sliding angle along the parallel direction was approximately 3°, which was smaller than the SA along the vertical direction (12°). This method provides a new idea for preparation of superhydrophobic surfaces with bionic structures by laser technology. The method is simple, convenient, and low cost, which may become a general method for preparing superhydrophobic surface.

laser manufacturing, bionic, reed leaf, superhydrophobicity, polydimethylsiloxane (PDMS)

doi: 10.1360/N972018-00872